Enhancement on the generation of amplified spontaneous emission in thulium-doped silica fiber at 2 μm

M A Khamis*, K. Ennser

Electronic and Electrical Engineering, Swansea University, Swansea, UK.

Abstract

This paper investigates the generation of the amplified spontaneous emission (ASE) from thulium-doped silica fiber pumped at 1570 nm and 793nm. The developed model provides the ASE spectral power as functions of the fiber length and the pump power under single-pass forward (SPF) and double-pass bi-directional (DPB) pumping schemes. A broadband ASE source generated by solving a set of rate and propagation equations for 1570nm and 793nm pumping transitions, and taking into account the influences of cross relaxation (CR) in both pump schemes. Our findings reveal that for 1570nm pumping scheme, CR transition reduces the ASE generation. In addition, longer fluorescent lifetime increases the ASE power and reduces the pump power threshold. We numerically enhanced the generation of ASE broadband source from 1570nm/1570nm DPB pumping scheme. Our results show that 1570nm/1570nm DPB produces broadband ASE source with high slope efficiency and broader spectral bandwidth than that in SPF configuration. As a result, a 1570nm/1570nm DPB pump scheme is a suitable configuration to obtain higher power efficiency and a wider broadband source for the chosen thulium-doped silica fiber characteristics.

Keywords: Thulium-doped fiber, Amplified spontaneous emission, Silica host material, Numerical simulation, Cross relaxation process.

1. Introduction

Over the last few years, broadband sources near 2 μm have attracted the attention of many researchers. A broadband source at 2 μm demonstrates many useful characteristics, including high output power, high light brightness, good beam quality, compact structure and excellent spatial coherence. These characteristics make broadband sources at 2 μm suitable for use in a number of significant applications, such as remote sensing, gas sensing, medical surgery, materials processing and atmospheric lidar measurement [1-6]. In addition, high power and wideband sources are required in optical coherence tomography and fiber optic gyroscopes [7,8]. One effective way to generate this broadband source is by using the process of amplified spontaneous emission between $^3F_4$-$^3H_6$ transition in thulium-doped fiber. High broadband source efficiency can be obtained via diode pumping on the transition $^3H_6 \rightarrow {}^3H_4$ in combination with high concentration of thulium-doped silica fiber in order to take into account the cross-relaxation process [9,10]. Alternatively, the need for high doping concentrations can be avoided by using an in-band pumping scheme, which directly excites the upper laser level on the transition $^3H_6 \rightarrow {}^3F_4$. Nevertheless, high efficiencies can be achieved because of the much lower quantum defect associated with this pumping scheme [11]. However, in spite of the progress in the performance of thulium broadband sources the efficiency is still below those routinely provided from conventional thulium fiber laser oscillators. In order to get higher output power and broader spectra, different pump configurations have been proposed for Erbium doped fiber [12,13] however no systematic study has been done for Thulium doped fiber yet.

To better optimize the broadband source performance near 2 μm, it is necessary to develop a theoretical modeling and perform simulations. There are relatively few theoretical studies on ASE sources based on thulium-doped fiber (TDF) [14,15]. Hence, this paper proposes an ASE source modeling for both the single-pass forward (SPF) and double-pass bi-directional (DPB) configurations. We numerically investigate and compare ASE broadband source from 1570nm pumping scheme with that 793nm pumping scheme. Our model considers the cross-relaxation process until in case of 1570nm pumping scheme and this is the first time to our knowledge that taking into account this transition at 1570nm pump wavelength in generation of ASE source near 2 μm.

Figure 1 and 2 illustrate the schematic diagrams of the ASE source using pump configurations in SPF and DPB schemes, respectively. In Fig. 1, both output ends are employed to angle-polished facet. In Fig. 2, a flat cleave is putted to extract ASE power from the end opposite the output end while angle-polished facet is employed at output end of the fiber.

In the DPB configuration, a single-ended operation is obtained by making the reflectivity of one end much higher than the other. At the same time, the product of the two-ended reflectivity should be low enough to suppress parasitic lasing [16,17]. The relationship between the reflectivity of both ends and ASE output powers are described by the following equation:

* Corresponding author. Tel: +00-000-000-0000; fax: +00-000-000-0000;
E-mail: author@domain.com

$$\frac{P_1}{P_2} = \left(\frac{1-R_2}{1-R_1}\right)\sqrt{\frac{R_1}{R_2}} \quad (1)$$

Here P_1 and P_2 represent the ASE output power of end 1 and 2, respectively. R_1 and R_2 are the effective feedback reflectivity at end 1 and 2, respectively. The end 1 is opposite to the ASE output end 2.

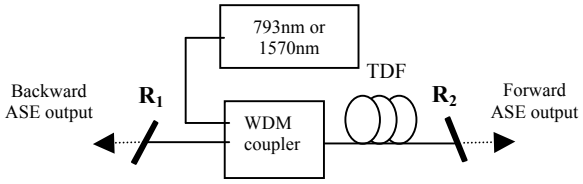

Fig. 1. A schematic of the ASE source using a single pass forward (SPF) pump configuration.

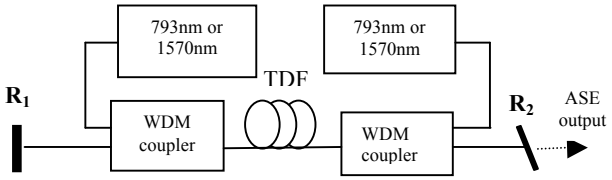

Fig. 2. A schematic diagram of the ASE source using a double pass bi-directional (DPB) pump configuration.

2. Modeling of ASE generation

A theoretical model of ASE generation using SPF and DPB pumping schemes are presented. The investigation into ASE spectral power is achieved by solving the rate and propagation equations. Figure 3 shows the four lowest energy manifolds of trivalent thulium ions which contain 1570nm and 793nm pumping transitions. According to the chosen pumping scheme, a separate numerical model is constructed. The model takes into account the wavelength-dependent absorption and emission cross-sections for the single and dual pump configurations.

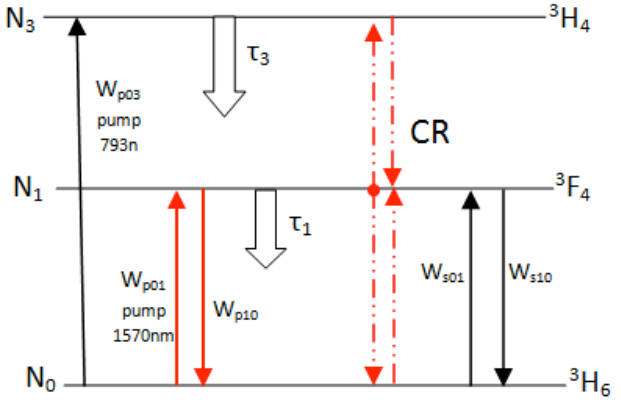

Fig. 3. Simplified energy level diagram of Tm^{3+} ions. The pump and laser transitions are indicated as solid arrows together with the energy transfer mechanisms. The dash lines represent the cross-relaxation process CR.

2.1 1570nm pumping scheme

Based on Jackson [18] and including ASE and the cross-relaxation transitions [19], the rate equations of thulium energy levels are established as the following:

$$\frac{dN_3(z,t)}{dt} = -\frac{N_3(z,t)}{\tau_3} - C \quad (2)$$

$$\frac{dN_1}{dt} = w_{p01}N_0(z,t) - w_{p10}N_1(z,t) - \frac{N_1}{\tau_1} - w_{s10}N_1(z,t) + w_{s01}N_0(z,t) + \frac{\beta_{31}N_3(z,t)}{\tau_3} + 2C \quad (3)$$

$$N_0(z,t) = N_T - N_1(z,t) - N_3(z,t) \quad (4)$$

Where C is the cross-relaxation process and is given by:

$$C = k_{3101}N_0(z,t)N_3(z,t) - k_{1310}N_1^2(z,t) \quad (5)$$

Here N_T is the Tm^{3+} ion concentration and set to be a constant. τ_1 is the spontaneous lifetime of the $^3F_4$ level; N_0, N_1 and N_3 are the population densities of the $^3H_6$, $^3F_4$ and $^3H_4$ levels, respectively; w_{p01} is the pumping rate from $^3H_6$ to $^3F_4$ and w_{p10} represents the de-excitation of the $^3F_4$ level; w_{s10} is the stimulated emission rate from $^3F_4$ to $^3H_6$, and w_{s01} is the stimulated absorption rate from $^3H_6$ to $^3F_4$. The expressions of w_{p01}, w_{p10}, w_{s10} and w_{s01} can be obtained from:

$$w_{p01} = \frac{\lambda_p \Gamma_p}{hcA_{core}}\sigma_a(\lambda_p)(p_p^-(z) + p_p^+(z)) \quad (6)$$

$$w_{p10} = \frac{\lambda_p \Gamma_p}{hcA_{core}}\sigma_e(\lambda_p)(p_p^-(z) + p_p^+(z)) \quad (7)$$

$$w_{s01} = \frac{\lambda_s \Gamma_s}{hcA_{core}}\sigma_a(\lambda_s)[ASE^+(z) + ASE^-(z)] \quad (8)$$

$$w_{s10} = \frac{\lambda_s \Gamma_s}{hcA_{core}}\sigma_e(\lambda_s)[ASE^+(z) + ASE^-(z)] \quad (9)$$

Here λ_p is the wavelength of the pump light and λ_s is the signal light in vacuum; h is the Planck constant; c is the light speed in vacuum; A_{core} is the cross-section area of the fiber core; $\sigma_a(\lambda_p)$ and $\sigma_a(\lambda_s)$ are the absorption cross-sections of the pump light and the signal light, respectively; $\sigma_e(\lambda_p)$ and $\sigma_e(\lambda_s)$ are the emission cross-sections of the pump light and the signal light, respectively; $P^{\pm}(z)$ is the pump (corresponding to forward and backward) at position z; $ASE^+(z)$ and $ASE^-(z)$ are the forward and backward amplified spontaneous emission powers at position z; Γ_p and Γ_s are the confinement factors for the pump and the signal, respectively which are given by Eq. 10 [20].

$$\Gamma(\lambda) = 1 - \exp\left(-\frac{2a^2}{w^2}\right) \quad (10)$$

where w is the mode-width parameter of the fiber and a is the fiber core radius. The normalized frequency V of the fiber is given by:

$$V = \frac{2\pi aNA}{\lambda} \quad (11)$$

As V > 1.5 the mode-width parameter w of a step-index fiber can be determined by the normalized frequency V of the fiber as:

$$\frac{w}{a} = 0.632 + 1.478\ V^{-3/2} + 4.76\ V^{-6} \quad (12)$$

Meanwhile, the pump power distribution along the fiber length can be expressed by the following propagation equation:

$$\frac{dp_p^{\pm}}{dz} = \pm p_p^{\pm}(z)[\ \Gamma_p(\sigma_e(\lambda_p)N_1(z) - \sigma_a(\lambda_p)N_0(z)) - \alpha_p\ ] \quad (13)$$

The positive sign in (13) relates to the forward direction and the negative sign to the reverse direction. The distribution of the ASE forward and backward powers along the fiber length can be established as follows [1,15,21]:

$$\frac{dASE^{\pm}}{dz} = \pm ASE^{\pm}(z)[\ \Gamma_s(\sigma_e(\lambda_s)N_1(z) - \sigma_a(\lambda_s)N_0(z)) - \alpha_s\ ] \pm 2\sigma_e(\lambda_s)N_1(z)\frac{hc^2}{\lambda_s^3}\Delta\lambda \quad (14)$$

Where α_p is the pump intrinsic absorption and α_s is the signal intrinsic absorption for the thulium-doped fiber; $\Delta\lambda$ is the bandwidth of the ASE near 2 μm.

2.2 793nm pumping scheme

The general rate equations for the thulium energy levels at any point along the length of the fiber are given by [18]:

$$\frac{dN_3(z,t)}{dt} = w_{p03}N_0 - \frac{N_3(z,t)}{\tau_3} - C \quad (15)$$

$$\frac{dN_1(z,t)}{dt} = -w_{s10}N_1 + w_{s01}N_0 - \frac{N_1(z,t)}{\tau_1} + \frac{\beta_{31}N_3(z,t)}{\tau_3} + 2C \quad (16)$$

$$N_0(z,t) = N_T - N_1(z,t) - N_3(z,t) \quad (17)$$

The pump distribution can be established as follows:

$$\frac{dp_p^{\pm}}{dz} = \mp p_p^{\pm}(z)[\ \Gamma_p(\sigma_a(\lambda_p)N_0(z)) + \alpha_p\ ] \quad (18)$$

Note that the positive sign refers to the reverse direction and the negative to the forward direction. The term expressions of w_{s01}, w_{s10}, ASE^+ and ASE^- can be taken from 1570nm pump model.

In a steady state condition, the time derivatives of equations (2) to (4) for the 1570nm model and (15) to (17) for the 793nm model are set to zero. The fourth-order of Runge-Kutta method is applied to solve the differential equations of the pump and the ASE signals under the boundary conditions in Table 1. A relaxation method is used to solve the boundary conditions and to achieve the accuracy of less than 0.01% for the pump and the ASE powers [22]. The length of thulium-doped fiber (L) is divided into N segments along the z-direction. The values of the pump power and the ASE power propagating at both ends in the first segment (segment 0) are selected under the initial condition shown in Table 1. The power for the pump, the forward ASE and backward ASE at one end of a segment are applied as the input for the next segment until the last segment.

Table 1 Initial conditions

Initial condition	Explanation
$p_p^+(z=0)$ = Forward launched pump power.	Initial condition for 1570nm and 793nm pumps at z=0.
$p_p^-(z=L)$ = Backward launched pump power.	Initial condition for 1570 nm and 793nm pumps at z=L (only in DPB).
$ASE^+(z=0)=R_1\times ASE^-(z=0)$	Initial condition for forward amplified spontaneous emission at z=0.
$ASE^-(z=L)=R_2\times ASE^+(z=L)$	Initial condition for backward amplified spontaneous emission at z=L.

3. Model validation and verification

We compare our numerical results with the published experimental measurements in order to evaluate the accuracy and versatility of our model. We use a similar dual pump configuration to that in [23] which used a 791nm/1560nm dual pump scheme. As same with the experimental configuration, we use a commercial 50-cm long TDF (OFS TmDF200) pumped in bi-directional pumping configuration by two 250-mW pumps. For a fair validation, we use the same pumped wavelengths at 1560nm and 791nm. In addition, we take the influence of WDM couplers loss used in the experimental work. The actual pump powers launched into TDF are 230mW using a 791nm pump and 210mW using a 1560nm pump due to 0.3dB and 0.8dB loss of WDM couplers at these wavelengths. The only assumptions in the simulation are that the values for the intrinsic absorption at signal wavelengths and the isolator insertion loss.

Figure 4 illustrates the ASE spectra of the numerical simulation and the experimental measurements. In our simulation, we used 14 different wavelengths between (1650nm-2000nm). We have chosen these values according to the emission cross-section spectra [23] and the available experimental data. It is clearly seen a good agreement is achieved between the numerical and the experimental results with small variations due to the above assumptions. These give confidence on the proposed modelling and numerical simulations.

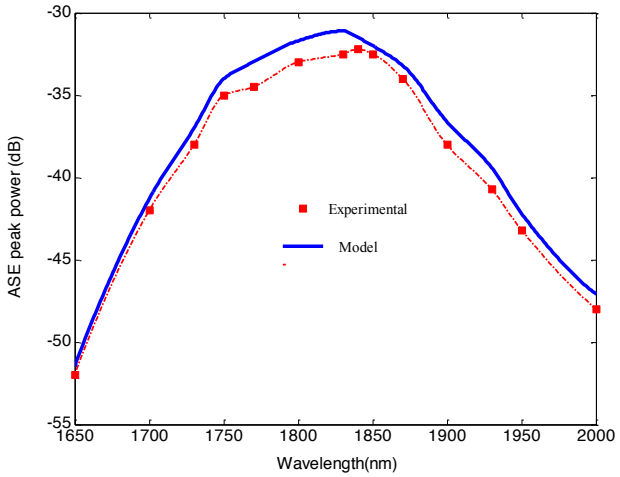

Fig. 4. ASE spectra for 793nm/1570nm pumping configuration for the numerical simulations and the experimental measurements.

4. Results and discussion

4.1 Single pass forward pumping configuration

A single-pass forward pump configuration is investigated with the reflectivity of both end equal -55 dB (R_1=R_2=3.16×10^{-6}) [1]. The design parameters used in our analysis are based on silica and were borrowed from Agger et al. [24], as summarized in Table 2, where the authors have measured all parameter values including the absorption and emission cross-section of the considered fiber, which is called Tm1.

Table 2: Values of numerical parameters

Symbol	Quantity	Value
N_T	Thulium concentration	7×10^{25} m^{-3} [14]
τ_1	Lifetime of level $^3F_4$	650 µs
τ_3	Lifetime of level $^3H_4$	12 µs
α_p	Intrinsic absorption at the pump wavelength	1.07×10^{-3} m^{-1} [18]
$\sigma_a(1570nm)$	Laser absorption cross section at *1570nm*	2×10^{-25} m^2
$\sigma_a(793nm)$	Laser absorption cross section at 793nm	6×10^{-25} m^2 [25]
$\sigma_a(\lambda_s)$	Laser absorption cross section at signal wavelength	See Ref [24]
$\sigma_e(\lambda_s)$	Laser emission cross section at signal wavelength	See Ref [23]
a	Fiber core radius	4.5 µm [14]
NA	Numerical Aperture	0.15 [14]
α_s	Intrinsic absorption at the signal wavelength	1.15×10^{-2} m^{-1} [18]
K_{0131}	Cross relaxation constant	1×10^{-23} m^{3}s^{-1} [25]
K_{1310}	Inverse cross relaxation constant	0.084 K_{0131} [18]

A MATLAB program was developed to evaluate the optimum thulium-doped fiber length for the 1570nm and 793nm pumping schemes. Figure 5 and 6 illustrate the theoretical prediction of the forward and backward ASE power and the residual pump power along a fiber length at 1570 and 793nm pumped wavelength, respectively. The pump power for both pump wavelengths is set to 500 mW, the fiber length equals 0.95m and 0.35m at 1570nm and 793nm pumped wavelength, respectively. The output ASE wavelength selected at 1840nm. The results show that the pump power distribution decreases along the fiber due to absorption and loss of the fiber until approach zero at a position of 0.9m at 1570 pumped wavelength and 0.3m at 793nm pumped wavelength. Moreover, the backward ASE is more powerful than the forward ASE as more than 30 mW is obtained compared to 19.5 mW in forward ASE for pump wavelength at 1570nm. In contrast to 0.27 mW and 0.38 mW in forward and backward ASE, respectively at pumped wavelength of 793nm. As a result, we notice that pumping at 1570nm is more powerful and efficient than at 793nm to build ASE broadband sources. In addition, the backward ASE should carry most of the output power as previously reported in [14].

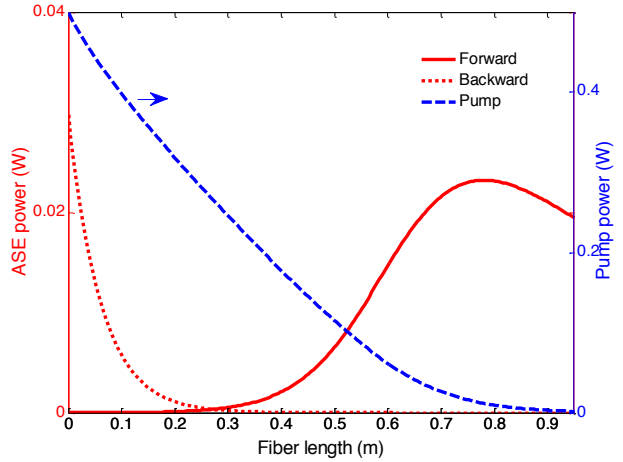

Fig. 5. Power distribution along the thulium fiber length for the pump, the forward ASE, and the backward ASE at 1570nm pumped wavelength.

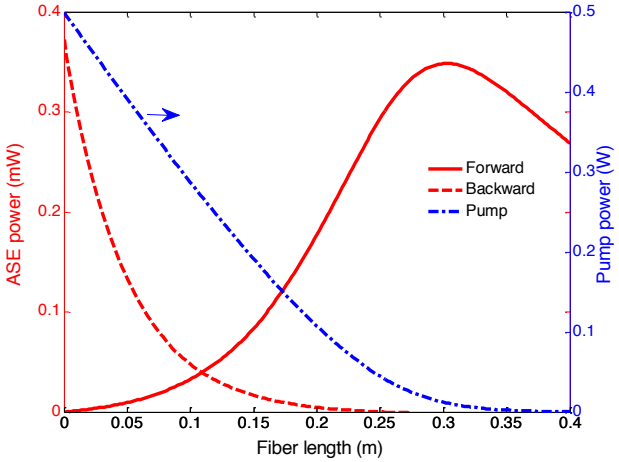

Fig. 6. Power distribution along the thulium fiber length for the pump, the forward ASE, and the backward ASE at 793nm pumped wavelength.

The output forward and backward ASE power as a function of TDF length is shown in Fig. 7 for 500 mW pumping at 1570nm and the signal wavelength at 1840nm. The output power increases rapidly with TDF length, and reaches the maximum value. The important point for output power consideration is to have a TDF length exceed the maximum value for a given pump power. Shorter or longer TDF length is an apparent disadvantage because of the lower output power. Thus, a 0.8m is the optimal TDF length to generate maximum ASE source at forward and backward.

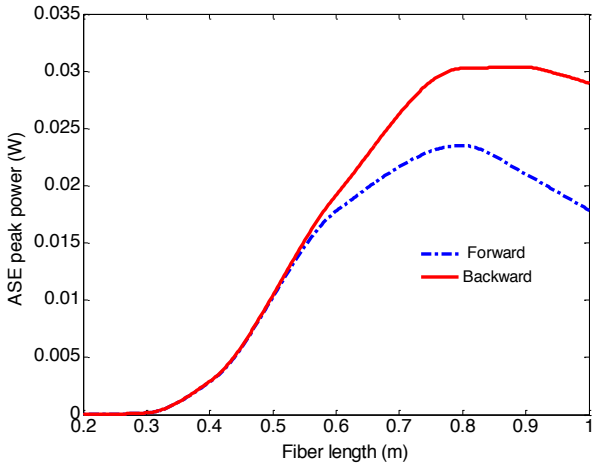

Fig. 7. Forward and backward ASE distribution versus thulium fiber length at 0.5W pump power and the signal wavelength of 1840 nm.

Figure 8 shows the forward and backward output power spectra of ASE for a 0.8 m TDF fiber length under the 500 mW pump power. The bandwidths of forward and backward ASE have full-width half maximums (FWHM) of 72 nm and 95 nm, respectively. The backward ASE has broader bandwidth than the forward ASE. In additional, high ASE power can be produced when the wavelengths are near the center of the emission cross-section curve of thulium-doped silica fiber.

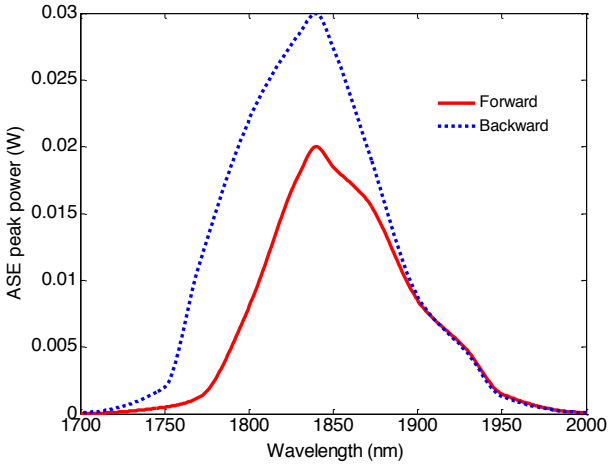

Fig. 8. Forward and backward power spectra of the SPF pumping scheme at total input pump power of 0.5W and 0.8m of fiber length.

We also investigate the effect of cross relaxation process in generation of ASE source pumped at 1570nm. Figure 9 shows the calculated ASE output at 1840nm wavelength under different input pump power with and without CR at a fiber length of 0.8. It is observed that for the same total pump power the maximum broadband ASE source should be reduced when considering CR. CR transition reduces the power efficiency of ASE source and this reduction will be larger at heavily thulium concentration. The reason is that the inverse cross relaxation K_{1310} acts to reduce the population inversion by transferring the Tm^{+3} ions from the upper energy level $^3F_3$ to the ground energy level $^3H_4$ [19]. Thus, it is necessary to avoid the selection of TDF with heavily levels of Tm^{3+} ions concentration.

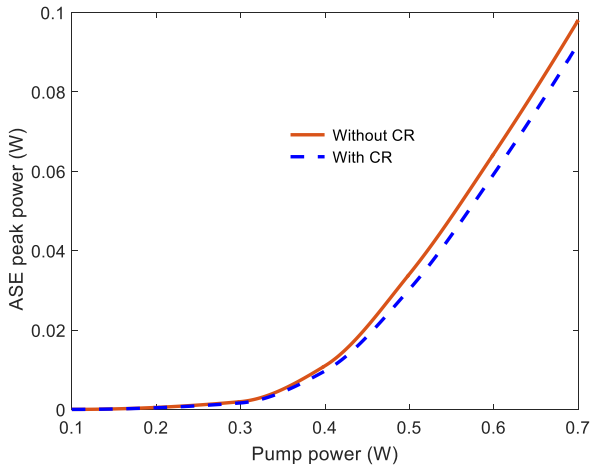

Fig. 9. ASE output power versus input pump power for SPF pumping scheme with and without cross relaxation (CR) effects.

The last parameter in our investigation is the effect of spontaneous life time of the metastable level (τ_1). We choose different values of τ_1 and intentionally fixed the other parameters in our simulation to focus only in the effect of the host material. Figure 10 shows the dependence of ASE

output power with the variation of the input pump power at different host material. It is clearly notice that longer τ_1 increases ASE power and reduces the threshold pump power.

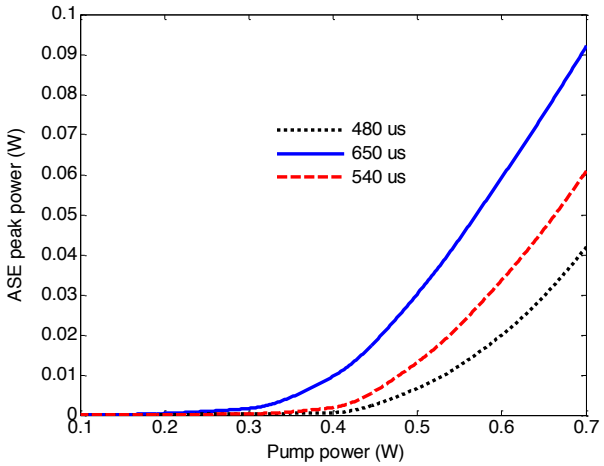

Fig. 10. ASE output power versus input pump power at SPF pump scheme with different fluorescence life time of $^3F_4$.

4.2 Double pass bidirectional pumping configuration

As a first step, we have optimized the single pass forward pumping configuration. Our investigation now deals with a double-pass bi-directional pumping scheme in order to increase both ASE power and spectra bandwidth. Within this configuration, we use 1570nm/1570nm DPB pumping scheme with each pump power of 0.25W and longer τ_1 at 650μsec. In addition, a 4% reflectivity is arranged in the opposite end of the output end (R_1=4%) and polished angle facet in the output end ($R_2=3.16\times10^{-6}$). This 4% reflectivity is sufficiently low to prevent the parasitic lasing over the using pump power.

Figure 11 illustrates the ASE spectrum of DPB pumping configuration under different TDF length. It is clearly seen that a 0.6m is the optimal fiber length at DPB scheme pumped at 0.5W. The reflectivity of 4% at DPB pumping scheme is enough to increase ASE power more than three times of the SPF configuration and also broadening the bandwidth to higher than 110nm. Figure 12 shows the variation of ASE output power with input pump power at 1840nm signal wavelength. The pump power threshold should be reduced at DPB configuration. In addition, the ASE output increases almost linearly after 0.3 W.

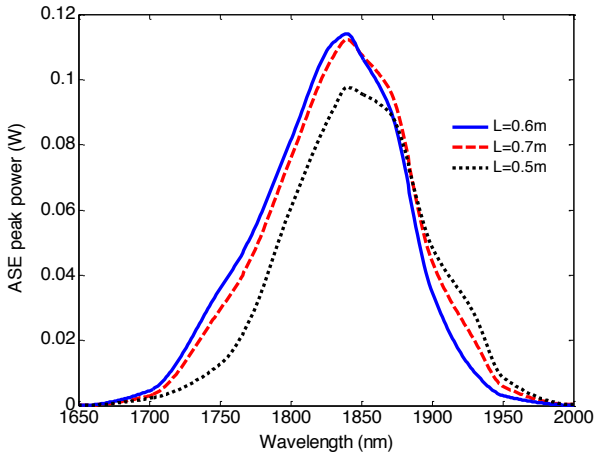

Fig. 11. Power spectra of the DPB pumping scheme at total input pump power of 0.5W.

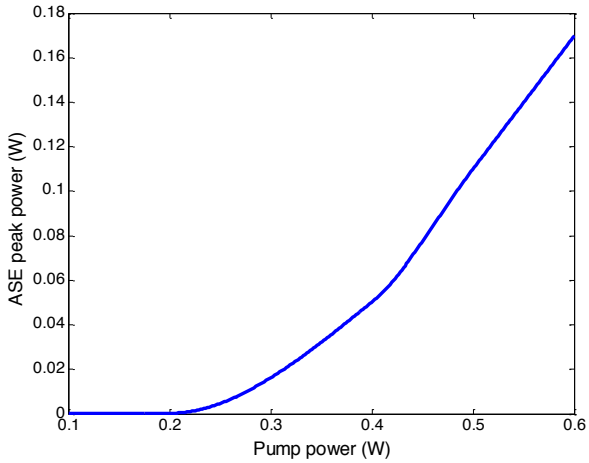

Fig. 12. ASE output power versus input pump power at DPB pumping configuration.

5. Conclusion

In summary, we have investigated the generation of a broadband ASE near 2 μm for a thulium-doped silica fiber with single-pass and double-pass bi-directional pumping schemes. We have presented a theoretical model of 2 μm ASE generation for thulium-doped fiber pumped at 1570nm and 793nm. A broadband ASE source performance is investigated by solving a set of rate and propagation equations for 1570nm and 793nm pumping transitions. The influence of cross relaxation effect is taken into account for both pump schemes. The model has been validated with previous experimental work. A good agreement has been achieved between our numerical findings and the experimental results, which gives confidence on the numerical simulations.

We have numerically compared ASE broadband source performance for single pass forward pumping scheme using 1570nm and 793nm. Our investigation shows that ASE power generation from 1570nm is more powerful than

793nm with same conditions. Also, it is clearly seen that backward ASE should carry most of the output power.

CR transition reduced the power efficiency of ASE source and this reduction is larger for higher thulium ions concentration. The inverse cross relaxation K_{1310} acts to reduce the population inversion by transferring the Tm^{+3} ions from the upper energy level $^3F_3$ to the ground energy level $^3H_4$ [19]. Thus, it is necessary to avoid the selection of heavily doped TDF. In addition, ASE power should be increased and threshold pump power reduced with longer spontaneous lifetime of metastable level so we have selected a host material with longer lifetime.

In the case of DPB, we have simulated several fiber lengths to maximize the ASE power. Our finding shows that 0.6m is the optimized fiber length for DPB pumping schemes. In addition, DPB configuration offers considerable high ASE power and wider spectrum bandwidth. The proposed ASE source design. Hence, is more suitable for applications that require high ASE power and broaden spectral bandwidth such as optical coherence tomography.

References

1. Z. Y. Hu, P. Yan, Q. Liu, E. C. Ji, Q. R. Xiao, and M. L. Gong, "High power single stage thulium doped superfluorescent fiber source," Appl. Phys. B. 118 (2014)101.
2. J. Li, Z. Sun, H. Luo, Z. Yan, K. Zhou, Y. Liu, and L. Zhang, "Wide wavelength selectable all-fiber thulium doped fiber laser between 1925 nm and 2200 nm," Opt. Express 22 (2014) 5387.
3. Z. C. Hsu, Z. S. Peng, L. A. Wang, R. Y. Liu, and F. Chou, "High power broadband all fiber super-fluorescent source with linear polarization and near diffraction-limited beam quality," Proc. SPIE 7004, 70044M (2008).
4. T. F. Morse, K. Oh and L. J. Reinhart, "Carbon dioxide detection using a co-doped Tm-Ho optical fiber," Proc. SPIE 2510 (1995) 158.
5. S. D. Jackson, A. Sabella, and D. G. Lancaster,"Application and development of high-power and highly efficient silica-based fiber lasers operating at 2μm," IEEE J. Sel. Top. Quantum Electron. 13 (2007) 567.
6. N. Sugimoto, N. Sims, K. Chan, and D. K. Killinger, "Eye-safe 2.1 μm Ho lidar for measuring atmospheric density profiles," Opt. Lett. 15 (1990) 302.
7. A. Halder, M. C. Paul, N. S. Shahabuddin, S. W. Harun, N. Saidin, S. S. A. Damanhuri, H. Ahmad, S. Das, M. Pal, and S. K. Bhadra, "Wideband Spectrum-Sliced ASE Source Operating at 1900-nm Region Based on a Double-Clad Ytterbium-Sensitized Thulium-Doped Fiber," IEEE Photonics J. 4 (2012) 14.
8. C. S. Cheung, J. M. O. Daniel, M. Tokurakawa, W. A. Clarkson, and H. Liang,"High resolution Fourier domain optical coherence tomography in the 2 μm wavelength range using a broadband supercontinuum source," Opt. Express 23 (2015) 1992.
9. K. Oh, "Broadband superfluorescent emission of the $^3H_4$ - $^3H_6$ transition in a Tm-doped multicomponent silicate fiber," Opt. Lett., 19 (1994) 1131.
10. D. Y. Shen, L. Pearson, P. Wang, J. K. Sahu, and W. A. Clarkson, "Broadband Tm-doped superfluorescent fiber source with 11 W single-ended output power," Opt. Express 16 (2008) 11021.
11. Y. H. Tsang, A. F. El-Sherif, and T. A. King, "Broadband amplified spontaneous emission fiber source near 2μm using resonant in-band pumping," J. Mod. Opt. 52 (2005) 109.
12. H. Wang, Y.-G. Li, S.-P. Chen, J.-P. Zhu, and K.-C. Lu,"Bandwidth broadening and efficiency enhancement of a double-pass forward L-band erbium-doped superfluorescent fibre source," J. Opt. A Pure Appl. Opt. 8 (2006) 897.
13. L. A. Wang and C. D. Su, "Modeling of a double-pass backward Er-doped superfluorescent fiber source for fiber-optic gyroscope applications,"J. Light. Technol. 17 (1999) 2307.
14. M. Gorjan, T. North, and M. Rochette, "Model of the amplified spontaneous emission generation in thulium-doped silica fibers," J. Opt. Soc. Am. B. 29 (2012) 2886.
15. G. Yu, J. Chang, Q. Wang, X. Zhang, Z. Liu, and Q. Huang, A theoretical model of thulium-doped silica fiber's ASE in the 1900 nm waveband," Optoelectron. Lett. 6 (2010) 45.
16. C. S. Cheung, J. M. O. Daniel, M. Tokurakawa, W. A. Clarkson, and H. Liang, "Optical coherence tomography in the 2-μm wavelength regime for paint and other high opacity materials," Opt. Lett. 39 (2014) 6509.
17. P. Wang, J. K. Sahu, and W. A. Clarkson, "Power scaling of Ytterbium-doped fiber superfluorescent sources," IEEE J. Sel. Top. Quantum Electron. 13 (2007) 580.
18. S. D. Jackson and T. A. King, "Theoretical Modeling of Tm-Doped Silica Fiber Lasers," J. Light. Technol. 17 (1999) 948.
19. M A Khamis and K Ennser "Theoretical Model of a Thulium-doped Fiber Amplifier Pumped at 1570 nm and 793 nm in the Presence of Cross Relaxation" J. of Lightwave Technology 34 (2016) 5675.
20. T. J. Whitley and R. Wyatt, "Alternative Gaussian spot size polynomial for use with doped fiber amplifiers," IEEE Photon. Technol. Lett.5 (1993) 1325.
21. M. A. Khamis and K. Ennser, "Model for a Thulium-Doped Silica Fiber Amplifier Pumped at 1558 nm and 793 nm," IJEAT 39 (2016) 76.
22. S. D. Emami, "Thulium-doped Fiber Amplifier, Numerical and Experimental Approach," New York: Nova Science Publishers, Inc. (2011).
23. J. Wang, S. Liang, Q. Kang, Y. Jung, S.-ul Alam, and D. J. Richardson, "Broadband silica-based thulium doped fiber amplifier employing multi-wavelength pumping," Opt. Express 24, (2016) 23001.
24. S. D. Agger and J. H. Povlsen, "Emission and absorption cross section of thulium doped silica fibers," Opt. Express14 (2006) 50.
25. M. Tao, Q. Huang, T. Yu, P. Yang, W. Chen, and X. Ye, "Cross relaxation in Tm-doped fiber lasers," *Proc. SPIE 8796, 2nd Int. Symp. Laser Interact. with Matter (LIMIS 2012)*, no. September 2015, p. 87961W, 2013.